The tide forecasting system for China coastal seas: A case study on the effect of tides on storm surge

Yifei Zhao[1], Zengan Deng[1,*], Jingsheng Zhai[1], Ting Yu[2], Hu Wang[1], Yu Cao[1], Yanbin Tong[1]

[1]*School of Marine Science and Technology, Tianjin University, Tianjin 300072, China*

[2]*National Marine Data and Information Service, Tianjin 300171, China*

[*]*Corresponding author: dengzengan@163.com*

Abstract

A Tide Forecasting and Visualization System (TFVS) is developed for providing the tidal information service for coastal regions of China. TFVS is capable of forecasting the tides (conducting harmonic analysis on the contrast) by invoking the T_TIDE package. Tide forecasting at 4 tidal stations has been carried out. Results show that the forecasted tides agreed well with the observations, which validates the accuracy and reliability of TFVS. Both forecasted and observed tides can be visualized and analyzed on TFVS. The realistic status of tides along China coastal region can be directly perceived/monitored on TFVS. In addition, TFVS provides reliable tidal data to the oceanographic community and further supports science-based decision-making (such as disaster mitigation) at local government levels. The storm surge in the coastal region of Jiangsu Province is carried out to detect the proportion between maximum astronomical tides and storm-induced water rise (storm surge) in storm situations. Using tidal data from TFVS, the average proportion of maximum astronomical tide to the highest total water level in Jiangsu Province is about 70%.

Keywords: Disaster mitigation; forecasting; information service; storm surge; tides.

1. Introduction

Gravitational forces from the moon and the sun act on seawater, resulting in periodical sea level elevation (water velocity) responses, which are called tides (tidal currents). Knowing the accurate fluctuations of tides and the resulting associated tidal currents accurately in the coastal region is essential for navigation, disaster mitigation and ocean management. Tides are usually studied by harmonic analysis. In classical harmonic analysis, tidal forcing is considered a finite set of sinusoids at specific frequencies (a sum of spectral lines). These frequencies are given by different combines of 6 fundamental frequencies associated with planetary motions (Godin, 1972). The fundamental frequencies represent the effects caused by the rotation of the earth, the orbit of the moon around the earth, the earth around the sun, periodicities in the location of lunar perigee, lunar orbital tilt and the location of perihelion. Pawlowicz *et al.* (2002) proposed a package of routines (T_TIDE) that can perform classical harmonic analysis with nodal corrections, inference and prediction functions.

In this work, a Tide Forecasting and Visualization System (TFVS) is developed with a Client/Server manner using java language. TFVS forecasts the tides by invoking the T_TIDE package/module. The forecasted results can be visualized and analyzed on TFVS. The system is capable of providing tidal information service in coastal region of China's seas.

Storm surge can be defined as the abnormal seawater rise (pile up) caused by strong atmospheric disturbances. It can inflict extreme havoc on coastal regions and their inhabitants (Wang, 2002). The total water level in a storm is combined by astronomical tide and storm surge. Thus, it is necessary to understand the ratio of astronomical tide to storm surge.

Jiangsu Province is adjacent to the Yellow Sea and East China Sea and is often affected by westerly, subtropical and other weather systems. Therefore, weather-induced oceanic disasters often occur. Storm surge from these systems can be extremely destructive (Wang *et al.*, 2011). According to historical statistics, the worst storm surges to ever affect Jiangsu Province were caused by typhoons (Luo *et al.*, 2014).

2. Basic theory of tide forecasting

For a component tide, its frequency (angular speed) σ is determined by 6 fundamental frequencies. They are the rotation of the earth (σ_r=14.492052 rad/h), the orbit

of the moon around the earth (σ_s= 0.549017 rad/h), the earth around the sun (σ_h= 0.041069 rad/h), periodicities in the location of lunar perigee (σ_p= 0.004642 rad/h), lunar orbital tilt ($\sigma_{n'}$= 0.002206 rad/h) and the location of perihelion ($\sigma_{p'}$= 0.000002 rad/h). Based on those 6 fundamental frequencies, the frequency of a certain component tide (angular speed σ) can be calculated by (Fang *et al.*, 1986):

$$\sigma = n_r\sigma_r + n_s\sigma_s + n_h\sigma_h + n_p\sigma_p +$$
$$n_{n'}\sigma_{n'} + n_{p'}\sigma_{p'}. \tag{1}$$

Coefficients before the 6 fundamental frequencies are called the Doodson number (Zhang *et al.*, 2011).

The tide level (ζ) is given by

$$\zeta = A_0 + \sum_k(H_k\cos(\sigma_k t + \theta_k + g_k)). \tag{2}$$

A_0 is mean water level, k marks the component tide, and σ_k is the angular speed that can be specified by Equation (1). H_k and g_k are respectively amplitude and phase lag is harmonic constants. θ is the original phase for the specified time.

Giving the harmonic constants, tide elevation can be predicted from Equation (2). In contrast, the harmonic constants for a certain location can also be derived by using a time series of tide (water level) observation.

3. Validation of tidal forecasting performed by TFVS

Fluctuations of tides at 4 tide stations were predicted using T_TIDE module in TFVS. The stations in this study were LYG [34.75°N, 119.48°E], LSI [32.13°N, 121.62°E], KMN [28.08°N, 121.28°E] and ZPO [21.58°N, 111.81°E] (Figure 1). The tidal observations of these stations were collected for 2011 and 2012.
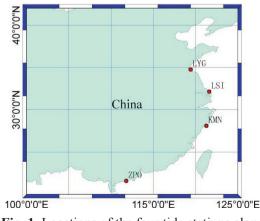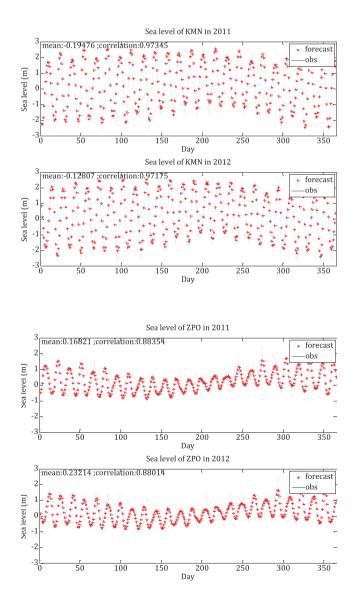

Fig. 1. Locations of the four tide stations along China's coastline

Figure 2 shows that the tidal prediction technique gives a good forecasting of the water level compared with the observations at KMN, LYG and LSI stations in both 2011 and 2012. At ZPO station, due to the missing data, the blue line (observations) is out of shape, but the prediction generally reshaped the correct curve. It is important to mention that the deviation between the prediction and measurements is relatively obvious, probably because of wind conditions or other meteorological effects. Figure 2 also gives the prediction skills based on a comparison of the predicted and observed tidal amplitudes in terms of statistical measures such as the correlation coefficient. It provides an overall view on the prediction skill of the present study for a particular station. One can find a consistent, good correlation for all the stations.
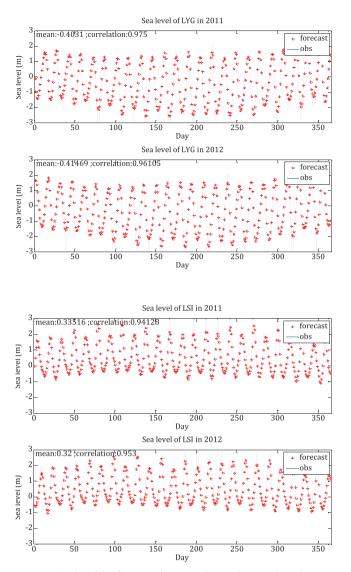
Fig. 2. Tide forecasting results and associated observations at four tide stations (KMN, ZPO, LYG and LSI) in China's seas. Red stars represent forecast time series. Blue curve is observed tidal series.

4. Architecture of TFVS

TFVS was developed using Java language with a Client/ Server manner. The technical scheme of TFVS is similar to that of a radar information service system developed by Deng *et al*. (2016). It has three layers: the Server Part (SP), Application Middleware (AM) and Client Part (CP) (Figure 3). The AM serves as a communication interface and a basic service platform. It incorporates three parts which are World Wind Java (WWJ), the Web Map Service (WMS), and ArcGIS packages. The link and communication between CP and SP are realized via AM. CP is constructed based on a three-dimensional geographical information software WWJ, which is one of the AMs. CP consists of 3 functional components, which are the Forecasting, Visualization and Output components,

for tidal harmonic analysis (as well as tidal forecasting), tidal data displaying/visualizing, and data files/figures/ animation generating, respectively. SP contains the Database and T_TIDE module. The Database mainly stores and manages the tidal observations, predicted tides as well as harmonic constants, whereas the T_TIDE module is in charge of harmonic analysis and tidal forecasting. In the harmonic analysis process, the T_TIDE module reads the tidal observations from the Database and sends the harmonic constants back to the Database. In contrast, in the tidal forecasting process, the T_TIDE module obtains the harmonic constants from the Database, and sends back the forecasted tides.
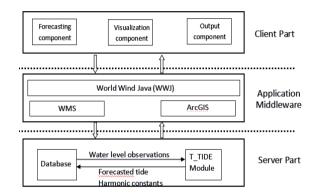

Fig. 3. Schematic diagram illustrating the architecture and components of TFVS

5. Application of TFVS to tidal information service

TFVS is also a Geographic Information System (GIS)-based three-dimensional globe visualization system. A variety of ocean data having geographic information or spatial coordinates can be loaded into and displayed by this system. Data consisting of points, profiles, fields, time serials, or three-dimensional grids all fit within the system. There are no restrictions on data temporal or spatial features. Such a system would allow users to navigate through space and time. They would have access to historical data as well as future predictions. In addition, it would support access and use of information by scientists, policy-makers, and the general public. The visualization covers multi-disciplines which are not limited to traditional physical oceanography, and it is also capable of displaying marine biological and geochemical observations. One important visualization function of TFVS is that it allows the ocean data to be spatially indexed, found and accessed through the user end. TFVS shows the ocean data as figures or animations, and users can view and download the files. For different data types, TFVS provides different visualization approaches.

The application of TFVS on the tidal information service from 4 tide stations is illustrated in Figure 4. A geo-browser virtual globe was hired to enhance the users' experience in accessing the tidal information. Both observed and forecasted tides can be displayed and compared on TFVS. Details of the tide series at 4 stations are shown in Figure 4. At the top part of the panel, the location of the tidal station is marked by a red flag on the 3D map. In addition to the metadata information from the tidal station, also listed (on the left) are the station name, geographic coordinates, administrative affiliation, sensor, observing parameters, etc. At the panel bottom is a plot showing the daily tidal fluctuations in near real-time. The red line gives the forecasted tides, while the green one shows the observations. Variable information (name, time, etc.) and statistics (e.g. mean tide height) are given on both sides of the plot. Besides browsing, users can download data files and plotted figures from the system. By using TFVS, the features and real time status of tides in the coastal region of China's seas can be monitored by data managers.
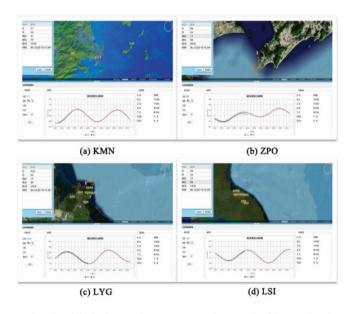

(a) KMN   (b) ZPO

(c) LYG   (d) LSI

Fig. 4. Tide information at KMN (a), ZPO (b), LYG (c) and LSI (d) visualized on TFVS

6. Case study of storm surge in the coastal region of Jiangsu Province

In this section, characteristics of a storm surge (storm-induced water rise) at two tidal stations (LSI and LYG) in Jiangsu Province were investigated. The time spans of the tidal data output from TFVS are from 1998-2012

at LSI and 1995-2012 at LYG. Data from China's Meteorological Administration's Tropical Cyclone Database (*tcdata.typhoon.org.cn*) were also collected for storm surge forecasting (Ying *et al*., 2014).

The storm surge forecasting method can be divided into two kinds; one is empirical forecasting and the other is numerical forecasting (Feng *et al*., 1999). The empirical forecasting mainly uses regression analysis to establish the empirical equation, including typhoon elements and tidal level at a specific location. This method has a high degree of accuracy for single station forecasts but can only be used for a particular location. The empirical equation adopted here is

$$\zeta = A\Delta P_0(1 - e^{-r_0/r}) + C \quad , \tag{3}$$

where ζ is the maximum storm-induced water rise. $\Delta P_0 = P_\infty - P_0$, $P_\infty = 1008$hPa, P_0 is the center pressure. r_0 is the radius of the maximal wind speed, which is taken as an average of 0.64, and r refers to the distance between the typhoon center and the station, expressed in latitude (Yin *et al*., 2015). A and C are coefficients to be determined. (In this study, they are fitted using the typhoon information listed in Table 1.)

Table 1. Typhoon elements

Station	Tropical cyclone	Maximum storm surge/cm	Center pressure /hPa
	0012 Prapiroon	129	970
	0205 Rammasun	170	980
	0509 Matsa	82	980
	0515 Khanun	52	995
LSI	0713 Wipha	78	995
	1105 Meari	76	985
	1109 Muifa	139	965
	0012 Prapiroon	75	970
	0908 Morakot	62	998
LYG	1109 Muifa	89	980
	1210 Damrey	178	988

Several typical typhoons with large influences on LSI and LYG have been collected and analyzed. Table 1 lists the typhoon data downloaded from the China Meteorological Administration's tropical cyclone database (*tcdata.typhoon.org.cn*).

The typhoons that affect LSI station can be divided into two types according to their travelling path. The first type is 'northward after landing' (such as No.0012, No.0205, No.1105 and No.1109), and the second one is 'northward without landing' (such as No.0509, No.0515 and No.0713). The empirical equations for the two types of typhoon in LSI can be fitted through Equation 3 by using the typhoon information in Table 1. These are northward after landing type:

$$\zeta = 3.3 \times \Delta P_0 (1 - e^{-0.64/r}) + 59, \tag{4}$$

northward without landing type:

$$\zeta = 8.0 \times \Delta P_0 (1 - e^{-0.64/r}) + 66. \tag{5}$$

The typhoon that mainly affects LYG station is 'northward without landing'. The corresponding empirical equation fitted is

$$\zeta = 6.5 \times \Delta P_0 (1 - e^{-0.64/r}) + 49. \tag{6}$$

Table 2 gives the deviations between the measured maximum storm surge and the corresponding values hind-casted by the empirical Equations 4, 5, 6 proposed in this study.

The difference between the measured and hind-casted values of the maximum storm surge is insignificant. The deviation at LSI station varied between 8 and 40 cm, which is acceptable, as mentioned in the literature and previous studies relevant to this topic (Gao *et al.*, 2014). The average relative error at LSI station was 16.6%, which was a value even smaller than that of previous studies. The maximum and minimum errors at LYG station were 1 and 12cm, respectively. The average relative error at LYG station was only 7.7%, which shows the excellent reliability of the empirical equation. This proves that the empirical equations proposed in this paper are capable of providing a valuable reference for future storm surge forecasting.

Table 2. Comparison of measured and hind-casted values of maximum storm-induced water rise (storm surge)

Station	Tropical cyclone	Measured maximum storm surge/cm	Hindcast maximum storm surge/cm	error	Relative error
LSI	0012 Prapiroon	129	147	18	14.0%
	0205 Rammasun	170	130	40	23.5%
	0509 Matsa	82	74	8	9.8%
	0515 Khanun	52	70	18	34.6%
	0713 Wipha	78	68	10	12.8%
	1105 Meari	76	87	11	14.5%
	1109 Muifa	139	149	10	7.2%
	Average			16	16.6%
LYG	0012 Prapiroon	75	86	11	14.7%
	0908 Morakot	62	63	1	1.6%
	1109 Muifa	89	77	12	13.5%
	1210 Damrey	178	176	2	1.1%
	Average			6.5	7.7%

In order to further understand the role of astronomical tides in the storm surge situations at the two stations, we obtained the maximum astronomical tide level by tidal harmonic analysis (tide forecasting). Severe disaster may occur if a maximum storm surge collides with the highest astronomical tide. Hence, it is necessary to figure out the ratio between them.

Table 3. Comparison of astronomical tide and storm surge

Station	Tropical cyclone	Measured maximum storm surge (cm)	Highest astronomical tide (cm)	Proportion of astronomical tide in total water level	Average Proportion
	0012 Prapiroon	129	303	70.1%	
	0205 Rammasun	170	226	57.1%	
	0509 Matsa	82	210	71.9%	
LSI	0515 Khanun	52	137	72.4%	65.1%
	0713 Wipha	78	116	59.7%	
	1105 Meari	76	152	66.7%	
	1109 Muifa	139	186	57.6%	
	0012 Prapiroon	75	222	74.7%	
	0908 Morakot	62	199	76.2%	
LYG	1109 Muifa	89	205	69.7%	70.1%
	1210 Damrey	178	264	59.7%	

Table 3 shows that the average proportions of maximum astronomical tide to the highest total water level (sum of tide and storm surge) at the two chosen stations were almost similar (65.1% at LSI and 70.1% at LYG). The maximum and minimum values at LSI were 72.4% and 57.1%, respectively, whereas the corresponding ones at LYG were 76.2% and 59.7%. According to these statistics relating to percentage in Figure 5, we can generally estimate the maximum total water level caused by a typhoon. This can be done by combining the astronomical tide and storm surge, which is of significant importance to disaster forecasting, warning, and mitigation.
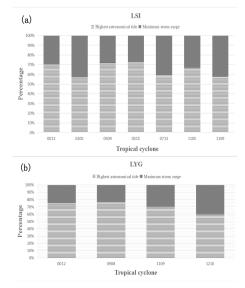

Fig. 5. The proportions of astronomical tide and storm surge in total water level in storm cases at LSI (a) and LYG (b)

7. Conclusions

A Tide Forecasting and Visualization System (TFVS) was developed for the purpose of tidal information service in coastal regions of China. T_TIDE was integrated as a module in TFVS for tide forecasting and harmonic analysis. Results of the tide forecasting experiments at 4 stations indicate that the forecasted tides are in good agreement with the observations. This validates the reliability of TFVS in tide forecasting and harmonic analysis in coastal regions of China's seas.

The case study of storm surge in the coastal region of Jiangsu Province was also performed. The empirical equations for forecasting two types of typhoon storm surge were fitted with the typhoon information. The forecasted storm surge data in this work was even more accurate than previous results given by other authors. Also, the highest total water level in a storm can be generally estimated by combining both the astronomical tide and storm surge. The data show that the average ratio of maximum astronomical tide to the highest total water level is about 70%. This information is important to disaster warning, mitigation, and management.

References

Deng, Z., Zhang, A., Zhai, J., Yu, T., Wu, S., *et.al.* (2016). An operational radar current observing and data service platform in the East China Sea. Acta Oceanologica Sinica, **35**(11): 1-7.

Fang, G., Zhen, W., Chen, Z., *et.al.* (1986). Analysis and forecast of tide and tidal currents. Ocean Press: Beijing, China. Pp. 9-10, in Chinese.

Feng, S., Li, F. & Li, S. (1999). Introduction to Marine Science. Higher education press, Beijing, China. Pp. 231, in Chinese.

Gao, Q., Cao, B., Gao, X. & Xu, C. (2014). Analysis of the typhoon storm surge in the Nantong coastal zone and forecasting formulas. Marine Forecasts, **31**(1): 29-35, in Chinese.

Godin, G. (1972). The analysis of tides. University of Toronto Press: Toronto. Pp. 264.

Luo, F., Sheng, J., Pan, X. & Liu, Q. (2014). Studies and applications of refined storm surge model for Jiangsu coast. Journal of Nanjing University (Natural Science), **50**(5): 687-694, in Chinese.

Pawlowicza, R., Beardsleyb, B. & Lentzb, S. (2002). Classical tidal harmonic analysis including error estimates in MATLAB using T_TIDE. Computers & Geosciences, **28**: 929–937.

Wang, X. (2002). Lecture on storm surge forecasting knowledge. Marine Forecasts, **20**(3): 63-69, in Chinese.

Wang, K., Yin, Z. & Yin, J. (2011). Analysis on typhoon-induced storm surge vulnerability of China's coastal areas on rising sea level background. Journal of Tropical Oceanography, **30**(6): 31-36, in Chinese.

Ying, M., Zhang, W., Yu, H., Lu, X., Feng, J., *et.al.* **(2014).** An overview of the China Meteorological Administration tropical cyclone database. Journal of Atmosphere. and Oceanic Technology, **31**: 287-301. doi: 10.1175/JTECH-D-12-00119.1

Yin, S. & Chen, Q. (2015). Statistical forecast of storm surge research on sea area of Zhuhai. Water Conservancy Science and Technology and Economy, **2015**(11): 84-86, in Chinese.

Zhang, F., Wei, Z., Wang, X., Wang, Y. & Fang, G. (2011). Tidal harmonic analysis. Marine Sciences, **35**(6): 68-75, in Chinese.

نظام التنبؤ بالمد والجزر في سواحل البحار الصينية:
دراسة حالة عن تأثير المد والجزر على هبوب العواصف

¹ييفي تشاو، ¹زينجان دينج، ¹جينجشنج تشاي، ²تينغ يو، ¹هو وانغ، ¹يو تساو، ¹يان بين تونغ

¹كلية علوم وتكنولوجيا البحار، جامعة تيانجين، الصين

²الهيئة الوطنية لخدمة البيانات والمعلومات البحرية، تيانجين، الصين

الملخص

تم تطوير نظام التنبؤ بالمد والجزر (TFVS) لتوفير خدمة المعلومات عنهم في المناطق الساحلية الصينية. ويعتبر النظام قادر على التنبؤ بالمد والجزر بالاستناد إلى حزمة T_TIDE. تم تنفيذ التنبؤ بالمد والجزر في 4 محطات. وأظهرت النتائج أن التوقعات بالمد والجزر تتوافق تماماً مع الملاحظات التي تؤكد دقة وموثوقية نظام TFVS. يمكن تصور وتحليل حركات المد والجزر المُتوقعة والمرصودة بواسطة نظام TFVS. يمكن إدراك ورصد الحالة الواقعية للمد والجزر على طول المنطقة الساحلية الصينية مباشرة على TFVS. بالإضافة إلى ذلك، يوفر نظام TFVS بيانات موثوقة عن المد والجزر لمجتمع علم المحيطات (الاقيانوغرافي) ودعم المزيد من صنع القرار القائم على العلم (مثل التخفيف من الكوارث) للحكومات المحلية. تم تنفيذ عرام العواصف في المنطقة الساحلية لمقاطعة جيانغسو للكشف عن النسبة بين الحد الأقصى للمد والجزر الفلكي وارتفاع المياه الناجم عن العاصفة (عرام العواصف). باستخدام بيانات المد والجزر من TFVS، بلغ متوسط نسبة الحد الأقصى للمد والجزر الفلكي في أعلى مستوى إجمالي للمياه في مقاطعة جيانغسو حوالي 70 %.